



ELSEVIER

**Neurobiology
of Disease**

 www.elsevier.com/locate/ynbdi
 Neurobiology of Disease xx (2008) xxx–xxx

Sensory motor mismatch within the supplementary motor area in the dystonic monkey

E. Cuny, I. Ghorayeb, D. Guehl, L. Escola, B. Bioulac, and P. Burbaud*

Laboratoire de Neurophysiologie, UMR CNRS 5543, Université Victor Segalen, 146, rue Léo Saignat, 33076 Bordeaux, France

Received 16 October 2007; revised 17 December 2007; accepted 21 December 2007

Dystonia, a movement disorder characterized by abnormal postures, is associated in primary forms of the disease with subtle proprioceptive troubles and aberrant somatotopic representation in the somatosensory cortex (SC). However, it is unclear whether these sensory features are a causal phenomenon or a consequence of dystonia. The supplementary motor area proper (SMAp), a premotor cortical region, receives strong inputs from both the SC and basal ganglia. We hypothesized that disruption in sensory-motor integration within the SMAp may play a part in the pathophysiology of dystonia. Using a model of secondary dystonia obtained by 3-nitropropionic acid intoxication in rhesus monkeys, we first provide evidence that the SMAp was overexcitable in dystonic animals. Second, we show that proprioceptive inputs processed by SMAp neurons were dramatically increased with wider sensory receptive fields and a mismatch between sensory inputs and motor outputs. These findings suggest that abnormal sensory inputs impinging upon SMAp neurons play a critical role in the pathophysiology of dystonia.

© 2008 Elsevier Inc. All rights reserved.

Keywords: Dystonia; 3-NP; Electrophysiology; Single-unit recordings; Supplementary motor area; Monkey

Introduction

Dystonia is characterized by sustained muscle contractions causing twisting and repetitive movements or abnormal postures (Fahn and Eldridge, 1976). During voluntary movements, there is a lack of selectivity of motor command with an overflow of activity in muscles normally inactive in movement execution (Rothwell et al., 1983; Cohen and Hallett, 1988). However, several lines of evidence suggest that the disorders of movement in dystonia could be associated with disturbances in sensorimotor integration (Byl et al., 1996; Bara-

Jimenez et al., 1998; Elbert et al., 1998; Jahanshahi, 2000; Murase et al., 2000; Meunier et al., 2001; Muller et al., 2001; Lerner et al., 2004).

Imaging studies have demonstrated overactivity in the lateral prefrontal and premotor cortices during motor tasks in primary dystonia (Ceballos-Baumann et al., 1995b) but contradictory data have been reported concerning activation of the caudal supplementary motor area (SMAp) and primary sensorimotor cortex, depending on the clinical expression of dystonia at the time of scanning (Ceballos-Baumann et al., 1995a; Ibanez et al., 1999; Pujol et al., 2000; Lerner et al., 2004). These cortical changes are thought to result from an increased inhibition of the medial globus pallidus leading to an increased thalamic drive to premotor cortices (Bernardelli et al., 1998). However, the correlation between clinical status, metabolic and neuronal changes is still elusive. Single-unit recording techniques allow a direct and detailed approach to neuronal activity but limit investigation to one or a few brain regions. We decided to focus on the SMAp for several reasons: 1) within the motor loop, this cortical area is the main target of basal ganglia output projections (Alexander and Crutcher, 1990); 2) it is involved in postural control through its direct projections to regions of the primary motor cortex (Muakkassa and Strick, 1979) and spinal cord (Hutchins et al., 1988; Dum and Strick, 1996; Picard and Strick, 1996) controlling the proximal musculature; and 3) the SMAp receives dense sensory inputs from S1 (Rizzolatti and Fadiga, 1998).

Several questions remain unanswered concerning the role of the SMAp in the pathophysiology of dystonia. The first is whether this part of the mesial premotor cortex is overactive. To test this hypothesis we studied SMAp spontaneous single neuronal activity and microstimulation in normal and dystonic primates. The second question is whether the processing of sensory inputs is modified within SMAp. To date, enlarged somesthetic receptive fields have been reported in the sensory thalamus (Lenz et al., 1999; Blake et al., 2002) and primary somesthetic cortex (Bara-Jimenez et al., 1998; Elbert et al., 1998; Meunier et al., 2001) of patients with dystonia, but they have never been documented within the premotor cortical areas. Therefore, we extensively studied the response of SMAp neurons to passive limb movements in normal

* Corresponding author. Fax: +33 05 56 90 14 21.

E-mail address: Pierre.Burbaud@umr5543.u-bordeaux2.fr (P. Burbaud).

Available online on ScienceDirect (www.sciencedirect.com).

and dystonic sub-human primates in a model of secondary dystonia obtained by intramuscular chronic treatment with 3-nitropropionic acid (NP), a mitochondrial toxin that induces large and specific lesions of the striatum (Palfi et al., 1996, 2000; Brouillet et al., 1999; Ghorayeb et al., 2002).

Materials and methods

Animals

Two female rhesus macaques (*Macaca mulatta*) served as subjects in these experiments. The animals weighing 5 and 6 kg were housed in individual primate cages. They had *ad libitum* access to water and food and received daily a supplementation with various fruits. Their care was supervised by veterinarians skilled in the health care and maintenance of non-human primates, in strict accordance with the European Community Council Directive for experimental procedures in animals. The light–dark cycle (lights on from 7 a.m. to 7 p.m.), temperature (22 °C) and humidity (60%) were kept constant in the animal room. For several weeks before surgery, monkeys were trained daily to sit in a primate chair and to remain quiet during palpation of various parts of the body. Monkeys were regularly videotaped in their home cage or primate chair. These videos were used to assess the severity of movement disorder using the Burke–Fahn–Marsden scale (Burke et al., 1985). Electromyographic recordings were abandoned after several attempts because they were impossible to perform in good conditions in freely moving monkeys.

Model of dystonia

The model of dystonia was obtained by chronic intoxication with a mitochondrial toxin, 3-nitropropionic acid (3-NP, Sigma, Lyon, France), using a protocol previously described (Palfi et al., 2000). Briefly, the monkeys received daily intramuscular injections of 3-NP (twice daily, 10:00 a.m. and 7:00 p.m. for 7 days). The total daily starting dose was 10.0 mg/kg/day for both monkeys). Thereafter they received a weekly increment of 2.0 mg/kg until obvious neurologic signs were detected, at which point 3-NP intoxication was stopped.

Surgery and electrophysiological recordings

A stainless steel recording chamber (diameter 19 mm, Narishige, Tokyo, Japan) was implanted in the skull under general anesthesia (ketamine 10 mg/kg, PanPharma, Fougères, France; xylazine 2 mg/kg, Bayer Pharma, Puteaux, France; diazepam 0.5 mg/kg, Sigma, Lyon, France; atropine sulfate 0.2 mg/kg, Aguettant, Lyon, France). Supplemental doses of ketamine were given every hour to maintain a state of deep anesthesia. The central axis of the cylinder was stereotaxically positioned at A24 and L0 in both monkeys. A head-holder was embedded with dental cement around the chamber for immobilization during neuronal recording. Antibiotic (ampicillin, 100 mg/kg, DUPHAMOX L.A®, subcutaneously, Fort Dodge Santé Animale, Agen, France) and analgesic (paracetamol, 30 mg/kg, per os, UPSA, Agen, France) treatments were given for 1 week after surgery.

Animals were left to recover for 2 weeks before the start of the experiments. Then, they were placed daily for the 3 h of experimental sessions in a primate chair with their head restrained. Extracellular single-unit activity was recorded using tungsten microelectrodes insulated with epoxy (impedance 0.5–1.0 Mohms at

1 kHz) piloted with a microdrive (Narishige, MO-95, Tokyo, Japan). Neuronal activity was amplified (10–20 K), filtered (300 Hz–3 KHz) and displayed on an oscilloscope. A window discriminator was used to select spikes from background activity. These were then processed through an analogic-digital interface and stored on-line on a microcomputer. Neuronal activity was stored for 3 min of recording as the monkey sat quietly and then analyzed using the chart system soft (Chart 5.0, ADI instruments, USA).

Proprioceptive receptive fields (PRF) were defined as the pattern of neuronal responses to various passive limb movements. To this end, the different joints of the upper and lower contralateral limbs were gently displaced in various directions. Monkeys were trained to remain quiet during this procedure and were often rewarded with fruit juice. Accelerometers were fixed with straps on the mobile part of the explored limb. The latter was also manually maintained in contact with a capacitive proximity detector. These two systems were used to assess the onset and end of passive movements. Four joints of the upper (shoulder, elbow, wrist, fingers) and lower (hip, knee, ankle, toes) limbs were studied on both sides of the body. The effect of passive movements was tested for each joint in the following directions: shoulder (antepulsion, retropulsion, abduction, adduction, rotation), elbow (flexion, extension, pronation, supination), wrist (flexion, extension, cubital inclination, radial inclination), fingers (extension, flexion), hip (extension, flexion, abduction, adduction), knee (extension, flexion), ankle (extension, flexion) and fingers (extension, flexion). The effect of trunk and tail movement was also assessed. Neuronal activity was stored for 10 to 25 passive movements.

Intracortical microstimulation (ICMS) was performed at the end of each neuronal recording session at sites where PRF were found. A train of cathodal pulses (width 0.2 ms, train duration 150 ms at 300 Hz, intensity between 5 μ A and 200 μ A) was applied through a constant-current stimulator with the same electrode used for extracellular recordings. The threshold of current intensity giving observable movements was systematically recorded. By this method we mapped the motor-evoked response (MER) at each site of stimulation.

Neuronal recordings and ICMS were performed exactly at the same sites before and after the lesion in each animal.

Statistical analysis

Spontaneous firing frequencies between the normal and dystonic monkey were compared with a Mann–Whitney *U*-test. To characterize the pattern of discharge, we used a variability index (VI) corresponding to the rate of spike interval SD/spike interval mean calculated for each neuron (Escola et al., 2003). Neurons with a regular pattern had a low VI and those with an irregular pattern a high VI. A mean value of VI was calculated for neurons recorded in the normal and dystonic monkey, respectively, and compared with a Mann–Whitney *U*-test.

For each type of passive movement, a peri-stimulus histogram with respect to the onset of joint displacement was obtained by aligning neuronal activity on the signal delivered by the proximity detector or the accelerometer (Fig. 1). The mean discharge frequency was calculated during two epochs of 250 ms before and after passive limb movement. These two values were compared with a Wilcoxon signed rank test. Neuronal changes in relation with limb displacement were considered to be significant for $P < 0.05$.

During ICMS, movements were recorded if they were evoked repeatedly and clearly identified by two investigators. Their features

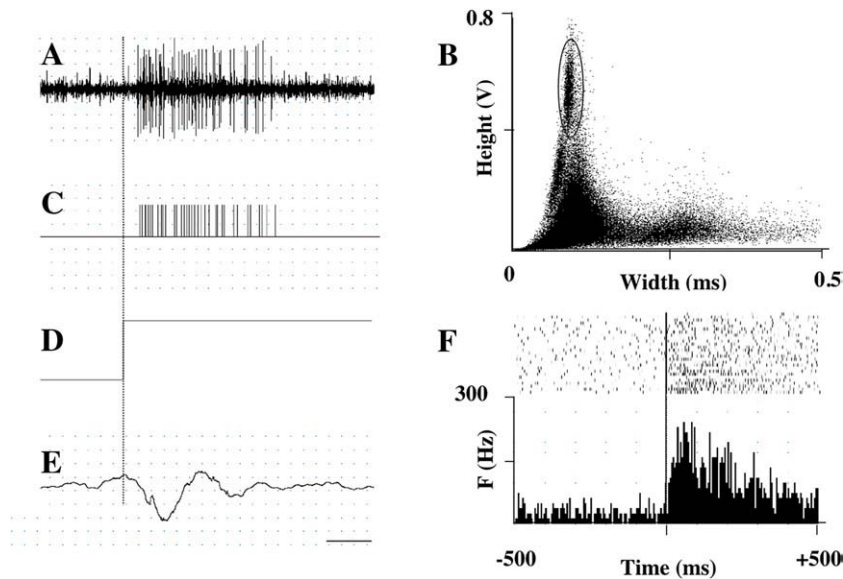


Fig. 1. Method for the analysis of responses to proprioceptive stimulation. (A) Direct trace of extracellular recording; (B) spike discrimination method based on shape recognition (spike height in ordinate, spike length in abscissa); (C) result of spike discrimination; (D) detection of movement onset (dotted line) with a capacitive proximity detector. In this example the detector is in close contact with the triceps sural at rest (bottom trace) before movement onset; (E) accelerometer; scale bar 100 ms; (F) peri-stimulus histograms aligned on the onset of knee extension.

in terms of joints involved and direction of movement were carefully monitored in order to map the motor-evoked response (MER). In addition, the threshold of motor-evoked responses at each site was determined by seeking the lowest intensity of current giving a visually evoked motor response. The microstimulation threshold between the normal and dystonic monkey was compared using a Mann–Whitney *U*-test.

Comparison of qualitative data between the normal and dystonic monkey was performed using χ^2 tests with $P < 0.05$.

Histopathology

At the end of the experiments, electrolytic lesions were made by applying an anodal direct current (20 μ A, 20 s) with the recording microelectrode. One week later, monkeys were deeply anesthetized (Nembutal, 100 mg/kg) and perfused through the ascending aorta with 500 ml of 0.9% saline, followed by 2 l of 4% paraformaldehyde in phosphate buffer (pH 7.4) as fixative. Limits of the recording chamber on the surface of the brain were marked and the brain was removed from the skull.

Location of recording tracks

Brains were frozen in -45°C isopentane, then stored at -80°C and cut into 10 μm cryostat coronal sections. One out of 5 sections was stained with cresyl violet and observed under a light microscope to control the location of recording tracks within the cortex. Reconstruction of the recording sites was based on the coordinates of each recorded cell with respect to marker lesions and, when possible, to the electrode track. Boundaries between the pre-SMA and SMAp were determined with information obtained by microstimulation, sulcal landmarks and cytoarchitectonic criteria. Reconstruction of recording sites showed that most tracks passed through the supplementary motor area. The location of each recorded neuron was carefully plotted in coronal sections of the medial wall. Neurons located in other bordering areas (pre-SMA, cingulate cortex, pri-

mary motor cortex) were discarded from data analysis. Careful examination of the cortex was performed to ensure that chronic recordings did not induce lesions due to repetitive tracks. To avoid this problem, the same tracks were never used on consecutive electrophysiological recording sessions.

Cytochrome oxidase histochemistry

Striatal mitochondrial oxidative metabolism was also studied using COx histochemistry as described by [Gonzales-Lima and Cada \(1998\)](#). Briefly, frozen sections were first incubated in cold buffered 0.5% glutaraldehyde in 0.1 M PBS, pH 7.4, followed by 4 baths of 0.1 M PBS, pH 7.4 with 10% sucrose. Pre-incubation was performed in Tris buffer containing 10% sucrose, 225 mg/l cobalt chloride and 0.5% dimethyl sulfoxide (DMSO). Sections were then incubated for 90 min at 37°C with automatic stirring in a dark oven in a previously oxygenated 0.5 g/l 3,3'-diaminobenzidine solution in 0.1 M PBS containing 75 mg/l of horse heart cytochrome C, 20 mg/l catalase, 0.25% DMSO and 5% sucrose. Post-fixation was done in buffered 10% formalin with 10% sucrose. Following incubation, slides were rinsed in phosphate buffer, dehydrated and coverslipped.

GFAP immunocytochemistry

Glial fibrillary acidic protein (GFAP) immunoreactivity was performed at the mid-striatal level to further assess the intensity of astroglial proliferation. After quenching for 10 min with 0.3% H_2O_2 , sections were rinsed, exposed for 48 h at room temperature to primary anti-GFAP rabbit serum [1:400 in 0.3% Triton X-100 (Sigma, France), BSAc 1/500 (Biovalley, Valbiotech, France) PBS], and then incubated (90 min) with biotinylated anti-rabbit antiserum (1:200, Vector, CA, USA). The reaction was revealed by the Vectastain ABC elite system (Vector).

Lesion surface quantification

Microscopic lesions were systematically sought in the cerebral cortex (particularly the temporal and frontal cortices), the basal

Table 1
Clinical assessment of dystonia

	Monkey # 1			Monkey # 2		
	Severity factor	Provoking factor	BFM score	Severity factor	Provoking factor	BFM score
Eyes	0	0	0	0	0	0
Mouth	0	0	0	0	0	0
Neck	0	0	0	0	0	0
Right arm	1	1	1	0	0	0
Left arm	0	0	0	0	0	0
Right leg	2	2	4	2	1	2
Left leg	2	1	2	3	4	12
Trunk	0	0	0	0	0	0
Total	–	–	7	–	–	14

Data correspond to the clinical scores rated on video sessions. The clinical items are adapted from the Burke–Fahn–Marsden scale (Burke et al., 1985).

ganglia, the cerebellum and the pons. Lesion surface quantification in the striatum was performed using an image analysis system (Mercator 3.10 B version, Explora Nova, La Rochelle, France). Fourteen COx stained sections per animal were analyzed along a rostro-caudal axis (7 sections for each hemisphere). For each section, both the caudate nucleus and the putamen were delineated to express the corresponding surface and the lesion, if present, was also contoured. Lesion percentage was deduced by plotting the lesioned surface to the total surface of either the caudate nucleus or the putamen. For each animal, lesion percentages were averaged and expressed as mean±SD.

Results

Primate model of secondary dystonia

Neurological signs due to 3-nitropropionic acid (3NP) intoxication occurred after 58 days in monkey # 1 (at 24.0 mg/kg/day) and after 52 days in monkey # 2 (at 22 mg/kg/day), leading to the immediate curtailment of 3NP intoxication. The onset of these signs was acute and was preceded by transient general weakness and slight somnolence. These neurological signs consisted of bilateral asymmetrical hind limb dystonia in both monkeys. There was no other type of movement disorders such as chorea, tremor, bradykinesia or hypotonia. Dystonia was even associated with mild hypertonia in monkey # 1. In both monkeys, dystonia predominated in the lower limbs with occasional diffusion to the right upper limb in monkey # 1. Dystonia was more severe and restricted to the lower limbs in monkey # 2 (Table 1). Although it was permanent during the course of the experiments, its severity could be increased by sensory stimuli (limb manipulation or tactile stimuli). However, it did not prevent the monkeys from eating or drinking in their home cage. Histopathological evaluation of the brain confirmed the presence of bilateral striatal lesions (Fig. 2) but there were no other lesions elsewhere in the brain either in the hippocampus, the neocortex, the cerebellum, basal ganglia (pallidum, substantia nigra, subthalamic nucleus) or brainstem.

Striatal lesions were revealed by COx histochemistry, which showed COx regional putaminal changes in activity that were more diffuse in monkey # 1 and encompassing the caudate nucleus (Figs. 2A, B). In monkey # 2, the lesions were larger but more

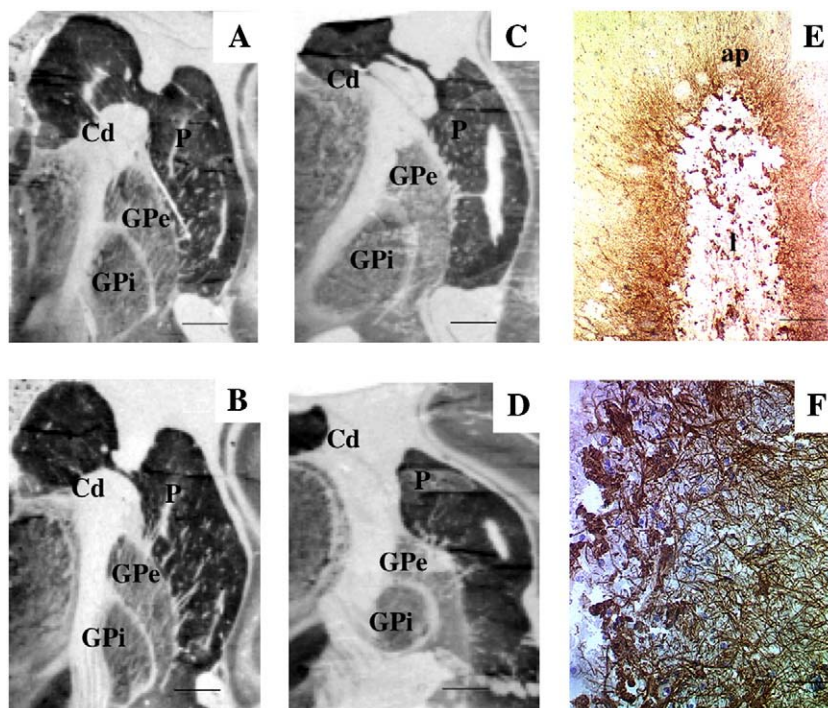


Fig. 2. Histological data. (A, B) Data of COx histochemistry in monkey M # 1; scale bar 1.25 mm; Cd: caudate nucleus; P: putamen, GPe: globus pallidus externalis, GPi: globus pallidus internalis. Diffuse necrosis was observed in the putamen and to a lesser extent in the caudate nucleus. (C, D) Data of COx histochemistry in monkey M # 2; same legend as in panel A. Focal necrosis predominated in the dorsolateral part of the putamen. (E) Glial fibrillary acidic protein (GFAP) immunoreactivity assessing the intensity of astroglial proliferation (ap) and revealing a loss of immunoreactivity in the core of the lesion (I), while the marginal area had abundant GFAP-labeled astrocytes; scale bar 20 μ m (F) enlarged view of GFAP reactivity; scale bar 5 μ m.

focal in the dorsolateral putamen (Figs. 2C, D). The sizes of the lesions (in % of putaminal volume) were 10 ± 3 in monkey # 1 and 7 ± 3 in monkey # 2, respectively. GFAP staining revealed a loss of immunoreactivity in the core of the lesion, while the marginal area had abundant GFAP-labeled astrocytes (Figs. 2E, F). Moreover, these astrocytes were widespread outside the lesion. Therefore, although the lesion represented on average less than 10% of the putamen volume, it was sufficient to induce clear dystonia in the lower limbs. Careful examination of the cortex in the region of the electrophysiological recordings revealed no significant lesions due to repetitive electrode tracks (not shown).

Neuronal excitability in the SMAp

A total of 1568 neurons recorded in the mesial frontal cortex of the two monkeys were analyzed. After histological reconstruction, 1312 were located in the SMAp, 98 in the pre-SMA, 104 in the cingulate cortex and 54 in the primary motor cortex. Statistical analysis was performed on a total of 767 SMAp neurons with a clear single-unit activity [440 neurons in the normal (187 in monkey # 1 and 253 in monkey # 2) and 327 in the lesioned monkey (220 in monkey # 1 and 107 in monkey # 2)]. Spontaneous neuronal activity was recorded at rest while the monkeys sat quietly in their primate chair. Examples of neuronal activity are given in Fig. 3 for neurons recorded with the same electrodes (Fig. 3A) or with two different electrodes (Figs. 3B, C). In most cases, neuronal activity was tonic and irregular. Bursts were infrequent both in the normal and lesioned monkey.

Basal firing frequencies were higher after (14.0 ± 13.5 Hz, $n=327$) than before (10.0 ± 11.2 Hz, $n=440$, $P < 0.0001$, Mann–Whitney *U*-test) 3-NP intoxication. The mean value of VI was higher in the dystonic monkey (2.2 ± 1.3 , $n=327$) than in the normal one (1.9 ± 1.0 , $n=440$, $P < 0.02$, Mann–Whitney *U*-test), indicating a more irregular pattern of discharge after 3-NP intoxication. During intracortical microstimulation (ICMS), the percentage of sites with motor responses was similar after (114/208 i.e. 55%) and before (146/247 i.e. 59%, χ^2 test, NS) the lesion. However, the threshold of stimulation needed to obtain a motor response was lower in the lesioned monkey (67.2 ± 60.1 μ A versus 84.0 ± 55.8 μ A, $P < 0.05$, Mann–Whitney *U*-test). Two types of motor responses were observed during ICMS: simple movements around a single joint and more complex movements involving two or more joints, which we termed polyjoint response. A large majority of motor-evoked responses involved a single joint both in the normal (116/146 i.e. 79%) and lesioned (94/114 i.e. 82%) monkey. The percentage of sites with polyjoint responses was similar in the two conditions (χ^2 test, NS), indicating that there was no diffusion of motor response after the lesion, i.e. movements induced by microstimulation did not involve more joints in the dystonic than in the normal monkey.

Response to proprioceptive inputs

The response of neurons to proprioceptive stimulation was studied on peri-stimulus histograms aligned on the onset of passive limb movement. Examples are shown for both normal (Figs. 4 and 5) and

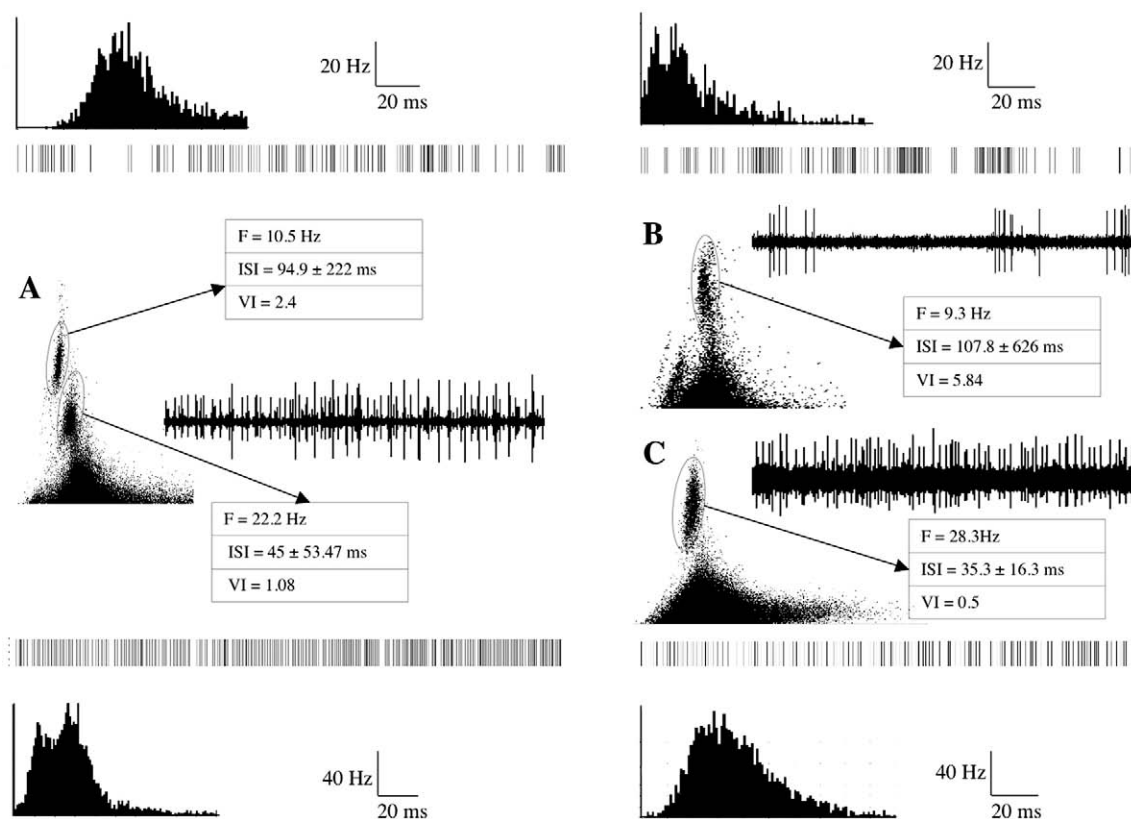


Fig. 3. Spontaneous neuronal activity in the SMAp. Different types of neuronal patterns are illustrated in this figure. (A) Two neurons recorded simultaneously with the same electrode. (B, C) Two neurons recorded with different electrodes. The direct recording trace, spike discrimination, a sample of raster display and the interspike interval histogram are represented for each neuron. Inserts give the mean firing frequency (F), the mean interspike interval (ISI \pm SD) and the variability index (VI) for each neuron.

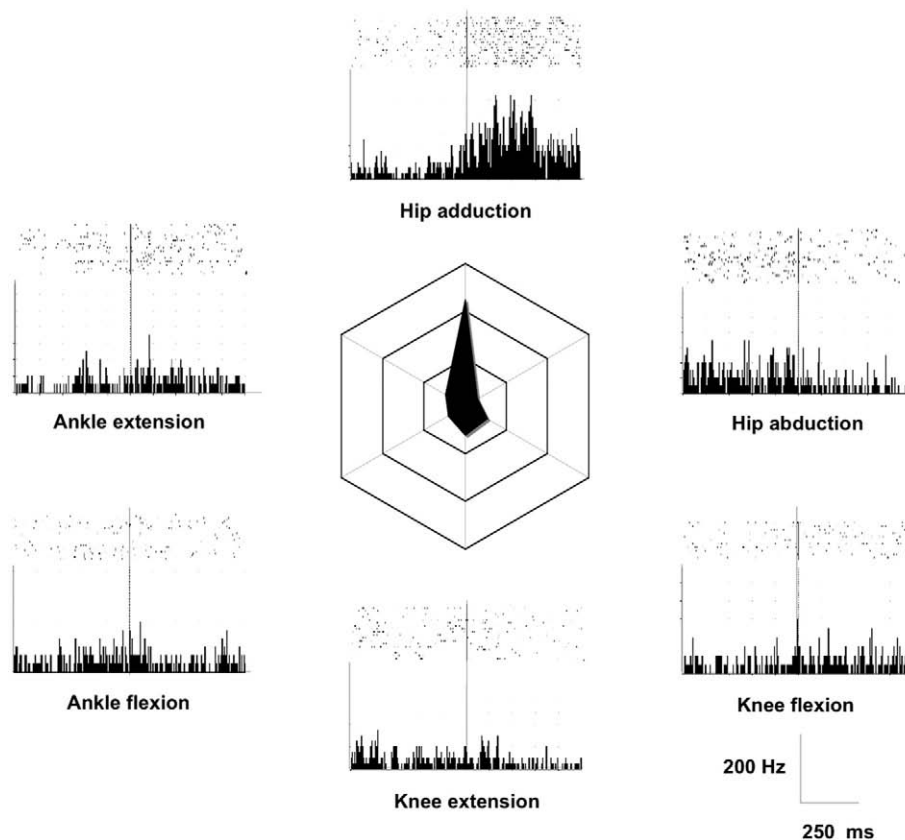


Fig. 4. Single-joint proprioceptive receptive field (PRF) with a directional specificity in normal monkey. Neuronal activity (top: raster display, bottom: peri-stimulus histogram) is aligned on the onset of joint displacement (vertical line) during passive joint mobilizations in different directions. Scale for ordinate (instantaneous firing frequency) and abscissa (time) are indicated in the right bottom. The central radar representation illustrates the mean firing frequency (radar scale 40 Hz for each band) during the 250 ms following passive movement. In this example, a significant change was observed only for hip adduction.

dystonic monkeys (Fig. 6). The percentage of neurons with proprioceptive receptive fields (PRF) was higher after (190/283 i.e. 67%) than before (190/380 i.e. 50%, $P < 0.0001$, χ^2 test) 3-NP intoxication. In particular, ipsilateral PRF, which were rare before the lesion (8/190, 4%), were dramatically increased in the lesioned monkey (76/190, 38%, $P < 0.0001$, χ^2 test). Neurons sensitive to passive mobilization of a single joint had single joint PRF, whereas those sensitive to passive mobilization of two or more joints had polyjoint PRF. In the normal monkey, the percentage of neurons with single joint PRF (145/190, 76%, Fig. 4) was higher than that of neurons with polyjoint PRF (45/190, 24%, Fig. 5), whereas the opposite was observed in the dystonic monkey (68/190, 36% versus 122/190, 64%, $P < 0.0001$, χ^2 test, Fig. 6).

We then sought whether there was a change in the direction sensitivity of SMAp neurons. Neurons responding to a joint displacement in one direction only, i.e. wrist flexion, were monodirectional, while those responding to joint displacement in two or more directions, i.e. wrist flexion, wrist extension and elbow flexion, were polydirectional. There was a clear increase in the number of neurons with polydirectional PRF in the dystonic monkey (146/190, 75%) versus the normal one (44/190, 20%, $P < 0.0001$, χ^2 test). Finally, we studied whether the firing frequency was different in neurons with polydirectional PRF, which was more frequent in dystonic monkeys, and in neurons with monodirectional PRF, which was common in normal monkeys. A higher firing frequency was found in the former (15.1 spikes/s vs. 11.5 spikes/s, $P < 0.0001$, Mann–

Whitney U -test), suggesting that the increase in firing rate observed in dystonic monkeys was due to the increase in proprioceptive inputs.

Finally, we found that the number of joints for PRF and MER recorded at the same site was similar in normal monkeys (Fig. 7, left). Conversely, the number was greater for PRF than for MER after the 3-NP lesion (Fig. 7, right).

Somatotopy in the SMAp

We wondered whether these variations in input/output coherence were associated with modifications in motor and sensory somatotopy. In the normal monkey, the motor representation of the upper limb was located in the rostral part of the SMAp and the lower limb representation in the caudal part, with the axis in an intermediate position (Fig. 8A, left). In the lesioned monkey, this pattern was disorganized, i.e. motor responses of the lower limb were also observed for ICMS of the SMAp rostral part (Fig. 8A, right). Proprioceptive somatotopy in the SMAp is illustrated in Fig. 8B. In the normal monkey (Fig. 8B, left), proprioceptive mapping was similar to motor mapping with a rostro-caudal organization (upper limb in the rostral part and lower limb in the caudal part with the axis between both), indicating a good spatial coherence between sensory inputs and motor outputs. However, as observed for motor somatotopy, considerable modifications in proprioceptive somatotopy

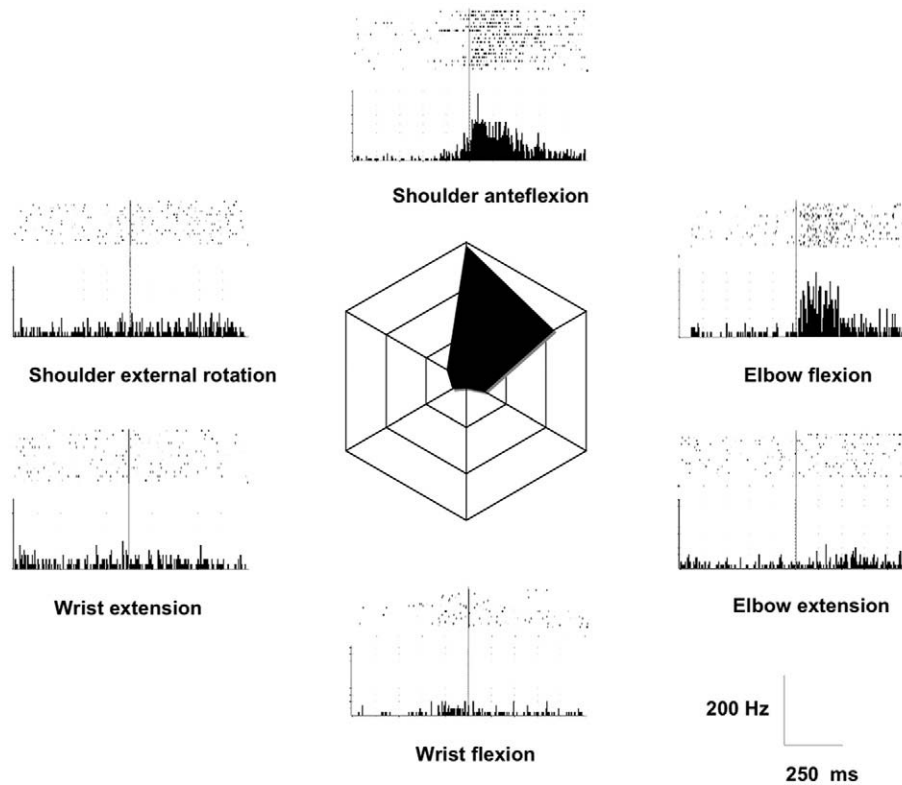


Fig. 5. Biarticular PRF with a direction specificity in normal monkey. Same legend as in Fig. 4. In this example, a significant change was observed for shoulder anteflexion and elbow flexion corresponding to a flexion movement of the upper limb.

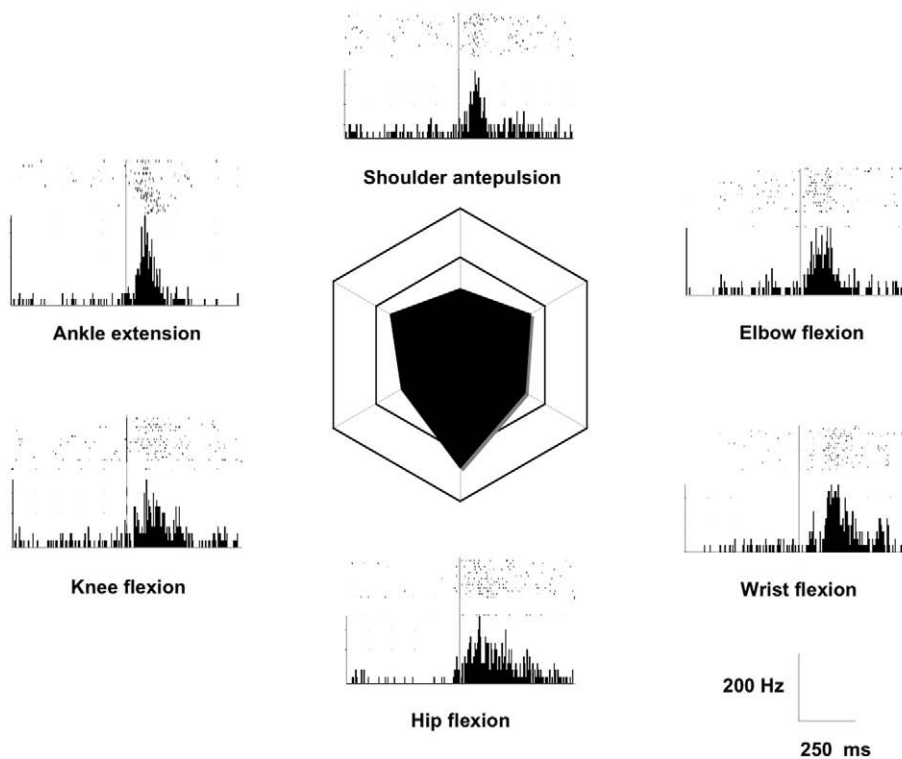


Fig. 6. Polyjoint PRF in dystonic monkey. Same legend as in Fig. 4. This neuron was activated by numerous passive movements both in the upper limb (shoulder antepulsion, elbow flexion, wrist flexion) and in the lower limb (hip flexion, knee flexion, ankle extension).

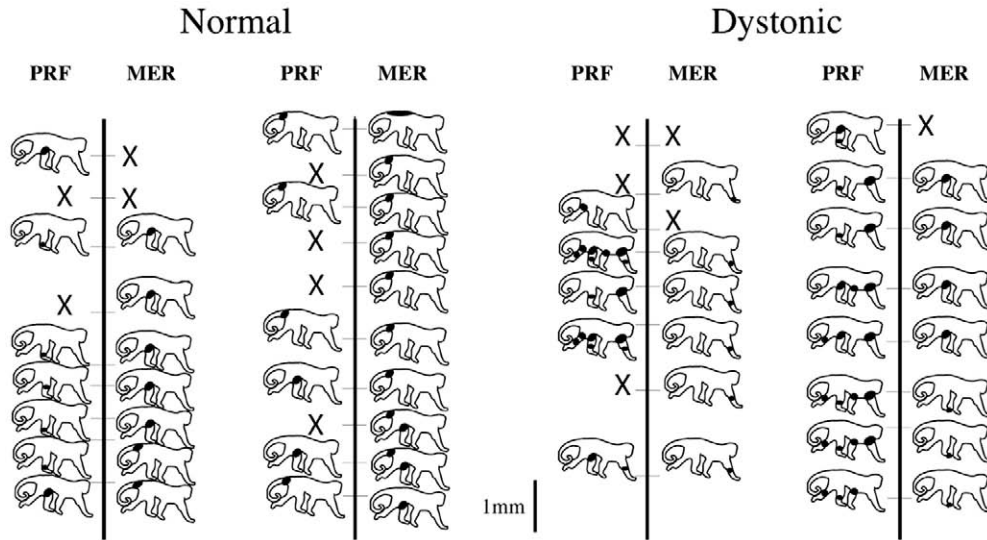


Fig. 7. Input/output coherence. The proprioceptive receptive fields (PRF) and motor-evoked responses (MER) observed at the same site before and after 3-NP intoxication are illustrated on four representative tracks as black areas on monkey figurines. X: no response recorded.

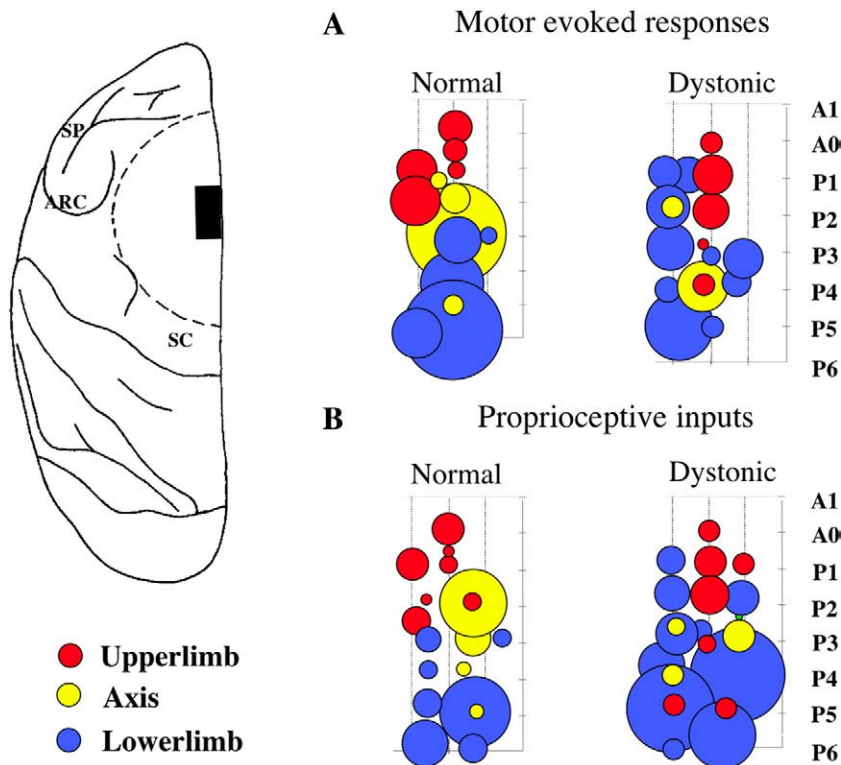


Fig. 8. Motor and sensory somatotopy in the SMAp before and after 3-NP intoxication. Left: top view of the brain; the recording chamber is represented as a dashed line and the area of recordings (SMAp) as a black rectangle; SP: principal sulcus; ARC: arcuate sulcus; SC: sulcus centralis. (A) Mapping of motor-evoked responses (MER); coordinates in mm [A: anterior, P: posterior vs. the ear bar (A0)]; red: upper limb; yellow: axis; blue: lower limb. For clarity, data of the two monkeys are pooled after careful anatomical reconstruction of recording tracks. In this representation the features (upper limb, lower limb or axis) of MER observed at each recording site are projected onto the cortical surface. The size of each circle is proportional to the number of joints where motor responses were evoked. (B) Mapping of proprioceptive inputs; same mode of representation as in panel A. In both cases (A and B), there was a tendency for diffusion of the lower limb representation towards the rostral SMAp region corresponding to the upper limb representation.

were found after the 3-NP lesion with a spreading of lower limb representation in the rostral part of the SMAp (Fig. 8B, right).

Discussion

In this model of secondary dystonia, the basal ganglia lesions observed after 3-NP intoxication mimicked those found in mitochondrial diseases such as Leigh disease, where progressive bilateral lesions of the caudate nucleus and putamen occur (Bernier et al., 2002). It is likely that the mechanism of 3-NP lesion is associated with an impairment of mitochondrial function, which in turn induces a metabolic stroke due to increased susceptibility of the putamen (Palfi et al., 1996, 2000; Brouillet et al., 1999; Ghorayeb et al., 2002). Although it was not possible to perform routine electromyographic recordings in our freely moving animals, the clinical features of dystonia resembled those reported in humans with secondary dystonia (Svetel et al., 2004), i.e. slow and sustained contractures corresponding to dystonic postures present at rest and worsened by sensory stimuli. These results are in line with the observation that a focal lesion of the dorsal putamen induces focal secondary dystonia (Bhatia and Marsden, 1994). In addition, the somatotopic representation of the foot, hand and face in the putamen predicts that a lesion in the dorsolateral part would more likely induce lower limb dystonia (Lehericy et al., 2003). The 3-NP model has been reported to induce other types of movements disorders such as chorea (Palfi et al., 1996; Brouillet et al., 1999), but pure dystonia similar to that observed in our animals has previously been found (Palfi et al., 2000; Ghorayeb et al., 2002). The type and extent of lesions observed after 3-NP lesions depend on the cumulative doses used for intoxications. It is likely that the limited lesions we observed in the striatum, the specific dystonic symptoms and the good clinical tolerance in our monkeys were due to the progressive intoxication schedule used, which was based on our previous experience with this model (Ghorayeb et al., 2002). The predominance of lesions in the striatum is probably due to its sensitivity to hypoxia (Palfi et al., 2000).

There is no doubt that dystonia is associated with profound changes in several subcortical and cortical regions involved in motor control. However, as previously stated, we decided to conduct a precise electrophysiological investigation focused on the SMAp because this premotor area is a critical link between the basal ganglia, the somatosensory cortex and the primary motor cortex. Our findings provide direct evidence for an abnormal excitability of the SMAp in secondary dystonia. Indeed, we observed an increase in neuronal discharge frequency associated with a decrease in the current threshold needed to evoke a motor response. However, neither the percentage of sites with motor responses to ICMS nor the percentage of sites with polyarticular motor responses was different between the normal and dystonic condition. Our microstimulation parameters were similar to those used by previous authors studying the SMAp (Luppino et al., 1991) and at these intensities induced simple myoclonic movements in different parts of the body. We cannot exclude that longer trains of stimulation might have induced more complex movements and posture, as previously observed in the primary and premotor cortex [for review see (Graziano et al., 2002)]. Even so, in similar conditions of stimulation, there was no diffusion of motor responses when comparing normal and dystonic monkeys, suggesting that the weight of connections between the SMAp and the primary motor cortex are functionally but not structurally modified. Because we did not perform systematic EMG recording during microstimulation, we cannot rule out that subtle

muscle contraction insufficient to induce visually detectable movement might have occurred. However, such movements, if any, would have been very discrete and probably of little functional significance.

Contrasting data have been reported concerning metabolic activity in the SMAp in dystonia. Initial studies found a decreased activity in the SMAp and primary motor cortex (M1) associated with overactivity in the pre-SMA and prefrontal cortex (Ceballos-Baumann et al., 1995b). However, overactivity of the SMAp seems to be observed when dystonia is clinically present during scanning both in primary (Pujol et al., 2000; Lerner et al., 2004) and in secondary (Ceballos-Baumann et al., 1995a) dystonia. Hence, in our experimental paradigm, the monkeys exhibited dystonia during neuronal recordings. Concurrently, there was an increased somatotopic motor representation of the lower limb area where dystonic signs predominated, associated with increased neuronal activity in this region. Since there are direct strong projections from the SMAp to M1 (Muakkassa and Strick, 1979), this phenomenon could contribute to the overactivity of M1 reported by previous authors in dystonic patients (Lerner et al., 2004).

The most salient finding of this study is the drastic increase in the processing of sensory inputs within the SMAp of the dystonic monkey. The number of neurons with proprioceptive receptive fields was increased after the 3-NP lesion and there was a clear spreading of receptive fields to several joints of the same limb or to other limbs, sometimes on the ipsilateral side of the body, a situation rarely observed before the lesion. Furthermore, PRF were less direction-specific in the dystonic than in the normal monkey, each SMAp neuron responding to more movements at each joint. A crucial question is why SMAp neurons process abnormal proprioceptive inputs. Several explanations may be put forward. The first is that it is the consequence and not the cause of the dystonic state, i.e. that dystonic postures might provide an increased volley of proprioceptive inputs to cortical neurons. However, in our monkeys, dystonia was restricted to the lower limbs whereas enlarged receptive fields were observed in most tested neurons receiving inputs from non-dystonic parts of the body, such as the upper limbs. Second, these abnormal inputs could be the result of aberrant cortical or subcortical inputs. Cortical inputs come from a wide spectrum of somatic sensory cortical regions such as areas 3a, 1 and 2 of the primary somesthetic cortex and area 5 of the parietal associative cortex (Jones and Powell, 1969; Jones et al., 1978). A disorganization of S1 somatotopy has been reported both in humans (Bara-Jimenez et al., 1998) and primate with occupational dystonia (Byl et al., 1996). Moreover, recent data obtained with voxel-based morphometry suggests that there could be an increased gray matter density in the S1 of dystonic patients (Garraux et al., 2004; Lerner et al., 2004) associated with S1 overactivity (Lerner et al., 2004). If information processing is altered in S1 in dystonia, it could also be the case in the SMAp which receive inputs from S1. Finally, subcortical inputs to the SMAp come from the basal ganglia (BG) through the motor thalamus. Hence, the proprioceptive fields commonly found in the internal pallidum, the subthalamic nucleus and in the thalamus are altered in dystonic patients (Lenz et al., 1999; Zhuang et al., 2004), suggesting a loss of focalization in information processing through the entire cortico-subcortical loops. However, it is unlikely that the BG play a direct role in somesthetic processing per se, but that they are more likely involved when sensory inputs are necessary for motor planning. This is in line with the observation that sensory disturbances are more evident in dystonic patients when the on-line movement requires a somesthetic feed-back (Hallett, 1995;

Abbruzzese and Berardelli, 2003). Further investigations are necessary to determine the origin of the disruption of sensory processing in the SMAp. In our model, this might require the simultaneous recording of SMAp, S1 and pallidal neurons in response to proprioceptive stimulation.

Can a model of mesial premotor cortical dysfunction in dystonia be established from these results? Our data provide direct proof of an overactivity of the SMAp associated with a diffusion of proprioceptive receptive fields in secondary dystonia. Consequently, the coherence between sensory inputs and motor outputs is modified. These increased sensory inputs with a low spatial selectivity could potentially play a part in SMAp overexcitability. The fact that dystonia was triggered in our monkeys by subtle sensory inputs that normally do not evoke a motor response is in line with this hypothesis. Such a dysfunction of sensorimotor integration within the supplementary motor area could lead to a disadaptation of motor planning. This model is in accordance with the increasing view that sensory processing is abnormal in dystonia (Abbruzzese and Berardelli, 2003). In turn, disorganized activity within the SMAp might induce the simultaneous recruitment of M1 columns controlling both agonist and antagonist muscles and leading to muscle co-contractions, a landmark of dystonia. However, since we used a model of secondary dystonia, we cannot rule out that the subtle dysfunction of basal ganglia occurring in primary dystonia, such as in DYT1, might be associated with different features of cortical dysfunction.

Acknowledgments

We wish to thank Ray Cooke for checking the English.

References

- Abbruzzese, G., Berardelli, A., 2003. Sensorimotor integration in movement disorders. *Mov. Disord.* 18, 231–240.
- Alexander, G.E., Crutcher, M.D., 1990. Functional architecture of basal ganglia circuits: neural substrates of parallel processing. *Trends Neurosci.* 13, 266–271.
- Bara-Jimenez, W., Catalan, M.J., Hallett, M., Gerloff, C., 1998. Abnormal somatosensory homunculus in dystonia of the hand. *Ann. Neurol.* 44, 828–831.
- Berardelli, A., Rothwell, J.C., Hallett, M., Thompson, P.D., Manfredi, M., Marsden, C.D., 1998. The pathophysiology of primary dystonia. *Brain* 121 (Pt 7), 1195–1212.
- Bernier, F.P., Bonch, A., Dennett, X., Chow, C.W., Cleary, M.A., Thorburn, D.R., 2002. Diagnostic criteria for respiratory chain disorders in adults and children. *Neurology* 59, 1406–1411.
- Bhatia, K.P., Marsden, C.D., 1994. The behavioural and motor consequences of focal lesions of the basal ganglia in man. *Brain* 117 (Pt 4), 859–876.
- Blake, D.T., Byl, N.N., Cheung, S., Bedenbaugh, P., Nagarajan, S., Lamb, M., Merzenich, M., 2002. Sensory representation abnormalities that parallel focal hand dystonia in a primate model. *Somatosens. Mot. Res.* 19, 347–357.
- Brouillet, E., Conde, F., Beal, M.F., Hantraye, P., 1999. Replicating Huntington's disease phenotype in experimental animals. *Prog. Neurobiol.* 59, 427–468.
- Burke, R.E., Fahn, S., Marsden, C.D., Bressman, S.B., Moskowitz, C., Friedman, J., 1985. Validity and reliability of a rating scale for the primary torsion dystonias. *Neurology* 35, 73–77.
- Byl, N.N., Merzenich, M.M., Jenkins, W.M., 1996. A primate genesis model of focal dystonia and repetitive strain injury: I. Learning-induced dedifferentiation of the representation of the hand in the primary somatosensory cortex in adult monkeys. *Neurology* 47, 508–520.
- Ceballos-Baumann, A.O., Passingham, R.E., Marsden, C.D., Brooks, D.J., 1995a. Motor reorganization in acquired hemidystonia. *Ann. Neurol.* 37, 746–757.
- Ceballos-Baumann, A.O., Passingham, R.E., Warner, T., Playford, E.D., Marsden, C.D., Brooks, D.J., 1995b. Overactive prefrontal and underactive motor cortical areas in idiopathic dystonia. *Ann. Neurol.* 37, 363–372.
- Cohen, L.G., Hallett, M., 1988. Hand cramps: clinical features and electromyographic patterns in a focal dystonia. *Neurology* 38, 1005–1012.
- Dum, R.P., Strick, P.L., 1996. Spinal cord terminations of the medial wall motor areas in macaque monkeys. *J. Neurosci.* 16, 6513–6525.
- Elbert, T., Candia, V., Altenmuller, E., Rau, H., Sterr, A., Rockstroh, B., Pantev, C., Taub, E., 1998. Alteration of digital representations in somatosensory cortex in focal hand dystonia. *Neuroreport* 9, 3571–3575.
- Escola, L., Michelet, T., Macia, F., Guehl, D., Bioulac, B., Burbaud, P., 2003. Disruption of information processing in the supplementary motor area of the MPTP-treated monkey: a clue to the pathophysiology of akinesia? *Brain* 126, 95–114.
- Fahn, S., Eldridge, R., 1976. Definition of dystonia and classification of the dystonic states. *Adv. Neurol.* 14, 1–5.
- Garraux, G., Bauer, A., Hanakawa, T., Wu, T., Kansaku, K., Hallett, M., 2004. Changes in brain anatomy in focal hand dystonia. *Ann. Neurol.* 55, 736–739.
- Ghorayeb, I., Fernagut, P.O., Stefanova, N., Wenning, G.K., Bioulac, B., Tison, F., 2002. Dystonia is predictive of subsequent altered dopaminergic responsiveness in a chronic 1-methyl-4-phenyl-1,2,3,6-tetrahydropyridine+3-nitropropionic acid model of striatonigral degeneration in monkeys. *Neurosci. Lett.* 335, 34–38.
- Graziano, M.S., Taylor, C.S., Moore, T., Cooke, D.F., 2002. The cortical control of movement revisited. *Neuron* 36, 349–362.
- Gonzales-Lima, F., Cada, M., 1998. Quantitative histochemistry of cytochrome oxidase activity. Theory, methods and regional brain vulnerability. Plenum press: New York.
- Hallett, M., 1995. Is dystonia a sensory disorder? *Ann. Neurol.* 38, 139–140.
- Hutchins, K.D., Martino, A.M., Strick, P.L., 1988. Corticospinal projections from the medial wall of the hemisphere. *Exp. Brain Res.* 71, 667–672.
- Ibanez, V., Sadato, N., Karp, B., Deiber, M.P., Hallett, M., 1999. Deficient activation of the motor cortical network in patients with writer's cramp. *Neurology* 53, 96–105.
- Jahanshahi, M., 2000. Factors that ameliorate or aggravate spasmodic torticollis. *J. Neurol. Neurosurg. Psychiatry* 68, 227–229.
- Jones, E.G., Coulter, J.D., Hendry, S.H., 1978. Intracortical connectivity of architectonic fields in the somatic sensory, motor and parietal cortex of monkeys. *J. Comp. Neurol.* 181, 291–347.
- Jones, E.G., Powell, T.P., 1969. Connexions of the somatic sensory cortex of the rhesus monkey. I. Ipsilateral cortical connexions. *Brain* 92, 477–502.
- Lehericy, S., Meunier, S., Garnero, L., Vidailhet, M., 2003. Dystonia: contributions of functional imaging and magnetoencephalography. *Rev. Neurol. (Paris)* 159, 874–879.
- Lenz, F.A., Jaeger, C.J., Seike, M.S., Lin, Y.C., Reich, S.G., DeLong, M.R., Vitek, J.L., 1999. Thalamic single neuron activity in patients with dystonia: dystonia-related activity and somatic sensory reorganization. *J. Neurophysiol.* 82, 2372–2392.
- Lerner, A., Shill, H., Hanakawa, T., Bushara, K., Goldfine, A., Hallett, M., 2004. Regional cerebral blood flow correlates of the severity of writer's cramp symptoms. *NeuroImage* 21, 904–913.
- Luppino, G., Matelli, M., Camarda, R.M., Gallese, V., Rizzolatti, G., 1991. Multiple representations of body movements in mesial area 6 and the adjacent cingulate cortex: an intracortical microstimulation study in the macaque monkey. *J. Comp. Neurol.* 311, 463–482.
- Meunier, S., Garnero, L., Ducorps, A., Mazieres, L., Lehericy, S., du Montcel, S.T., Renault, B., Vidailhet, M., 2001. Human brain mapping in dystonia reveals both endophenotypic traits and adaptive reorganization. *Ann. Neurol.* 50, 521–527.
- Muakkassa, K.F., Strick, P.L., 1979. Frontal lobe inputs to primate motor

- cortex: evidence for four somatotopically organized ‘premotor’ areas. *Brain Res.* 177, 176–182.
- Muller, J., Wissel, J., Masuhr, F., Ebersbach, G., Wenning, G.K., Poewe, W., 2001. Clinical characteristics of the geste antagoniste in cervical dystonia. *J. Neurol.* 248, 478–482.
- Murase, N., Kaji, R., Shimazu, H., Katayama-Hirota, M., Ikeda, A., Kohara, N., Kimura, J., Shibasaki, H., Rothwell, J.C., 2000. Abnormal pre-movement gating of somatosensory input in writer’s cramp. *Brain* 123 (Pt 9), 1813–1829.
- Palfi, S., Ferrante, R.J., Brouillet, E., Beal, M.F., Dolan, R., Guyot, M.C., Peschanski, M., Hantraye, P., 1996. Chronic 3-nitropropionic acid treatment in baboons replicates the cognitive and motor deficits of Huntington’s disease. *J. Neurosci.* 16, 3019–3025.
- Palfi, S., Leventhal, L., Goetz, C.G., Hantraye, T., Roitberg, B.Z., Sramek, J., Emborg, M., Kordower, J.H., 2000. Delayed onset of progressive dystonia following subacute 3-nitropropionic acid treatment in *Cebus apella* monkeys. *Mov. Disord.* 15, 524–530.
- Picard, N., Strick, P.L., 1996. Motor areas of the medial wall: a review of their location and functional activation. *Cereb. Cortex* 6, 342–353.
- Pujol, J., Roset-Llobet, J., Rosines-Cubells, D., Deus, J., Narberhaus, B., Valls-Sole, J., Capdevila, A., Pascual-Leone, A., 2000. Brain cortical activation during guitar-induced hand dystonia studied by functional MRI. *NeuroImage* 12, 257–267.
- Rizzolatti, G., Fadiga, L., 1998. Grasping objects and grasping action meanings: the dual role of monkey rostroventral premotor cortex (area F5). *Novartis Found. Symp.* 218, 81–95 (discussion 95–103).
- Rothwell, J.C., Obeso, J.A., Day, B.L., Marsden, C.D., 1983. Pathophysiology of dystonias. *Adv. Neurol.* 39, 851–863.
- Svetel, M., Ivanovic, N., Marinkovic, J., Jovic, J., Dragasevic, N., Kostic, V.S., 2004. Characteristics of dystonic movements in primary and symptomatic dystonias. *J. Neurol. Neurosurg. Psychiatry* 75, 329–330.
- Zhuang, P., Li, Y., Hallett, M., 2004. Neuronal activity in the basal ganglia and thalamus in patients with dystonia. *Clin. Neurophysiol.* 115, 2542–2557.